Porous SiC ceramics with dendritic pore structures by freeze casting from chemical cross-linked polycarbosilane

Fengdan Xue[a], Kechao Zhou[a,*], Ning Wu[a], Hang Luo[a], Xiaofeng Wang[a], Xuefan Zhou[a], Zhongna Yan[a], Isaac Abrahams[b], Dou Zhang[a,**]

State Key Laboratory of Powder Metallurgy, Central South University, Changsha 410083, China

[a] State Key Laboratory of Powder Metallurgy, Central South University, Changsha 410083, China

[b] Materials Research Institute, School of Biological and Chemical Sciences, Queen Mary University of London, Mile End Road, London, E1 4NS, UK.

*Corresponding author.

E-mail address: zhoukechao@csu.edu.cn.

**Corresponding author.

Tel /fax : +86 731 88877196

E-mail address: dzhang@csu.edu.cn.

Abstract: In this study, a commercial polycarbosilane (PCS) and divinylbenzene (DVB) were used as the preceramic polymer precursor and crosslinking agent, respectively to form porous silicon carbide (SiC) ceramics by freeze casting PCS/camphene/DVB solutions. Porous silicon carbide (SiC) with a dendritic pore structure and connecting bridges was obtained after pyrolysis at 1200 °C. The effects of DVB and PCS content on the rheological properties of the solution and the morphological characteristics and the compressive strengths of SiC ceramics were investigated. The use of DVB and the resulting chemical cross-linking yielded modified pore characteristics and much lower oxygen content in pyrolyzed SiC compared to the conventional thermal curing method. A compressive strength of 18.7 MPa was obtained for pyrolyzed SiC prepared with 20 wt. % PCS and a 0.2 DVB/PCS mass ratio.

Key words: Polycarbosilane, SiC, Divinybenzene, Freeze casting, Porous structure

1. Introduction:

Silicon carbide (SiC) ceramics have received much attention due to their excellent physical and chemical properties, including low density, high melting point, good thermal shock resistance, and excellent chemical inertness [1-5]. The theoretical density of SiC is 3.2 g/cm^3, which is favourable for fabrication of light weight structural materials [6]. Compared with its dense counterpart, porous SiC ceramics have larger surface areas and better thermal shock resistance, which are important properties for applications in catalyst supports [7-9], filters for hot gas [10] or molten metal [11, 12], membrane supports [13-15] and porous bio-implants [16, 17]. Therefore, porous SiC ceramic is one of the most widely used non-oxide ceramics in many industrial applications. The large band gap of SiC materials makes them suitable for harsh environment/high temperature sensor applications [18, 19], while porous SiC ceramics have good electromagnetic wave absorption properties and make them of interest as stealthy materials [20].

The applications of porous SiC ceramics are not only governed by the physical and chemical stabilities of SiC itself, but also the pore characteristics and the mechanical properties [21, 22]. Commonly, porous SiC is fabricated by powder processing, involving high temperature sintering up to 1900-2000 °C. It is worth noting that much effort has gone into the use of preceramic polymer precursors to generate porous silicon carbide materials, including sacrificial templating [23, 24], blowing [25, 26], etching [27], emulsions [28], aerogels [29], etc. Preceramic polymer

precursor derived ceramic processing is a simple method to produce high temperature ceramics with low sintering temperature and good formability [30-32], utilizing preceramic polymer precursors such as polysiloxane (PSO), polysilazane (PSZ), polycarbosilane (PCS) and polyborosilazane (PBSZ).

Freeze casting is a convenient and attractive method for fabricating porous materials [33]. The key parameters of freeze casting, such as cooling rate, solid loading and solvent etc., can be utilized to modulate the pore characteristics at multiple scales, ranging from micro [34, 35] to macro [36] levels in a one-step process, usually utilizing metal or ceramic powders as the suspension solids. Preceramic polymer precursors have also been employed in freeze casting for the fabrication of SiC ceramics. Yoon *et al*. [37] obtained porous SiC ceramics using oxidation-cured PCS preceramic polymer by freeze casting, while pyrolyzed ceramics showed amorphous phases of silicon oxycarbide (SiOC) and SiO_2. Naviroj *et al*. [38] obtained three types of pore networks of directionally aligned macroporous SiOC via freeze casting polysiloxane preceramic polymer using dibutyltin dilaurate as a cross-linking agent. However, much oxygen is introduced into porous SiC ceramics during the cross-linking process, leading to decreased compressive strengths of pyrolyzed SiC ceramics and complex deoxidation sintering processes for obtaining high purity SiC ceramics.

With this in mind, divinylbenzene (DVB) has been employed as cross-linking agent to fabricate porous SiC ceramics [39, 40]. In contrast, to other cross-linking agents, oxygen content was found to be much reduced in pyrolyzed SiC ceramics

prepared using DVB, because it is oxygen-free. We investigate here the effects of DVB and PCS content on the rheological properties of DVB/camphene/PCS solutions and the morphological characteristics and the compressive strengths of pyrolyzed porous SiC ceramics prepared by freeze casting.

.

2. Experimental details

2.1 Materials

PCS (SLF-PCS, M_W = 1000-2000 Da, Suzhou Champion Ceramic Fiber Co. Ltd., Jiangsu, China) was used as the preceramic polymer. The as-received solid PCS was crushed and sieved (180 μm) to give a fine powder to promote its dissolution behaviour in the solvent. Camphene ($C_{10}H_{16}$, purity = 95%, Shanghai Macklin Biochemical Co. Ltd., Shanghai, China) was used as the solvent and freezing vehicle. Divinylbenzene (DVB, mixed isomers, purity = 80%, Shanghai Aladdin biochemical Co. Ltd., Shanghai, China) was utilized as the cross-linking agent.

2.2 Processing

Firstly, the PCS powder was dissolved in hot camphene at 60 °C and stirred for 3 h to create a homogenous solution. DVB was then added to the homogenous solution and the cross-linking reaction carried out at 120 °C for 1h. DVB/camphene/PCS solutions were prepared with various PCS concentrations of 5-20 wt. % and DVB/PCS mass ratios of 0.1, 0.2, 0.4, and 0.6, corresponding to DVB/PCS monomer mole ratios of 0.045, 0.089, 0.179 and 0.268, respectively.

The warm cross-linked solutions were poured into a pre-heated cylindrical silicone mould, with an inner diameter of 10 mm and height of 15 mm and then placed on a copper plate sitting on a reservoir of liquid nitrogen. Thus freezing occurred vertically from the bottom of the mould upwards. Frozen samples were then removed from the mould and freeze dried in a vacuum chamber at 1 Pa (Scientz – ND, Ningbo Xingzhi biotechnology Co. LTD., Jiangsu, China) to allow for sublimation of camphene and unreacted DVB. The dried samples were then transferred to an alumina crucible and pyrolyzed at 1200 °C for 2 h in flowing argon to convert the PCS to the SiC ceramic. The combined procedures of freeze casting and pyrolysis are summarised in Fig. 1, with the cross-linking reaction given in Eqn. 1 [41, 42].

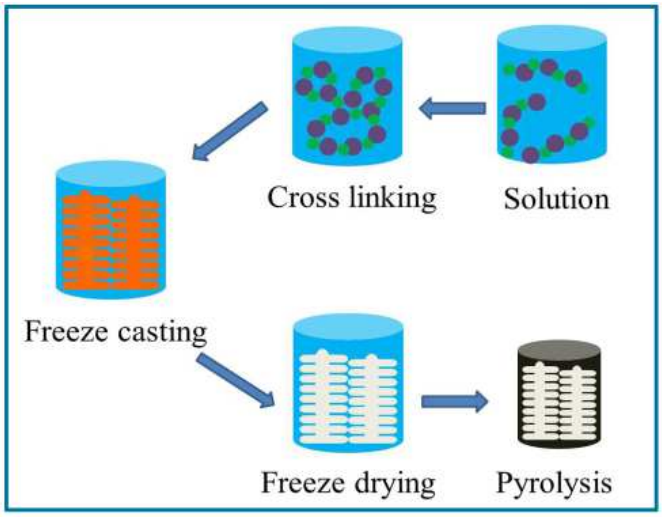

Fig. 1. Schematic illustration of preparation of porous SiC ceramics via freeze casting and pyrolysis of a preceramic cross-linked polymer

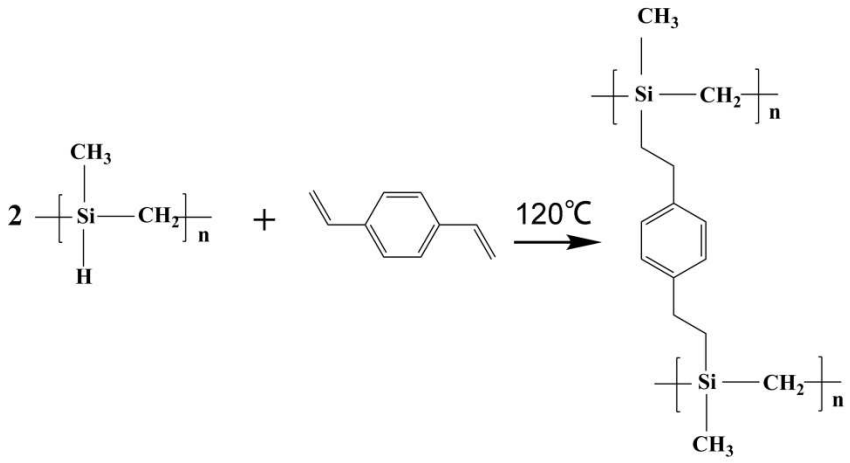

(Eqn. 1)

2.3 Characterization

X-ray powder diffraction was employed to characterize the crystalline phase of SiC ceramics after pyrolysis at 1200 °C using a Rigaku D/max 2550pc diffractometer (Rigaku, Japan) with monochromatic Cu Kα radiation (λ = 1.54178Å). Field emission scanning electron microscopy (FESEM, NOVA NANOSEM 230) with energy-dispersive spectroscopy (EDS, AZTec x-max 80) was used to observe the pore morphology and for analysing the composition of the pyrolyzed samples. Images were analysed using the Image J software [43]. Fourier transform infrared spectroscopy (FT-IR, Nicolet 6700) was performed on samples with different DVB content to assess the extent of cross-linking over the range 400 to 3000 cm^{-1}. The rheological properties of the solution were investigated using a rheometer (AR 2000, TA Instruments, USA) at 60 °C. The compressive strengths of pyrolyzed samples were tested using a universal mechanical testing machine (Instron 3369, USA). The open porosity (*P*%) of samples was measured by the Archimedes method and calculated using Eqn. 2.

$$P\% = \frac{m_3 - m_1}{m_3 - m_2} \times 100\% \quad \text{(Eqn 2)}$$

where m_1 is the dry mass of sample, m_2 is the mass of the sample when immersed in water and m_3 is the mass of the wet sample. Values presented are an average of three measurements.

3. Results and discussion

Fig. 2(a) shows the effect of DVB content on the viscosity of 10 wt. % PCS/ camphene solution at a shear rate of 0.1-500 s^{-1}, at 60 °C, after cross-linking for 1 h. The DVB/camphene/PCS solutions generally showed shear thinning behaviour and very low viscosity for all compositions, *i.e*. 1.9 × 10^{-3}, 2.2 × 10^{-3}, 9.9 × 10^{-2} and 0.120 mPa·s^{-1}, for samples with DVB/PCS mass ratios of 0.1, 0.2, 0.4 and 0.6, respectively at a shear rate of 100 s^{-1}. The DVB/camphene/PCS solutions were increasingly milky in appearance, with increasing DVB content. The viscosities showed relatively large difference between the solutions, with that of the 0.4 composition 45 times that of the 0.2 composition. The PCS chains are transformed to a network with increasing cross-linking, leading to a dramatic increase in viscosity [44]. Only small changes in viscosity are seen on further increasing the DVB/PCS mass ratio from 0.4 to 0.6, as the PCS gelation rate slows down in the later stages of cross-linking. Fig. 2(b) shows the effect of PCS content on the viscosity of samples containing a 0.2 DVB/ PCS mass ratio at shear rates of 0.1-500 s^{-1}, at 60 °C, after cross linking for 1h. The viscosity of the DVB/camphene/PCS solution increased with increasing PCS content, however, all compositions showed very low viscosity, with

values of 1.5 × 10^{-3}, 2.2 × 10^{-3}, 3.5 × 10^{-3} and 4.6 × 10^{-3} mPa·s^{-1} for compositions with PCS contents of 5, 10, 15 and 20 wt.% , respectively, at a shear rate of 100 s^{-1}.

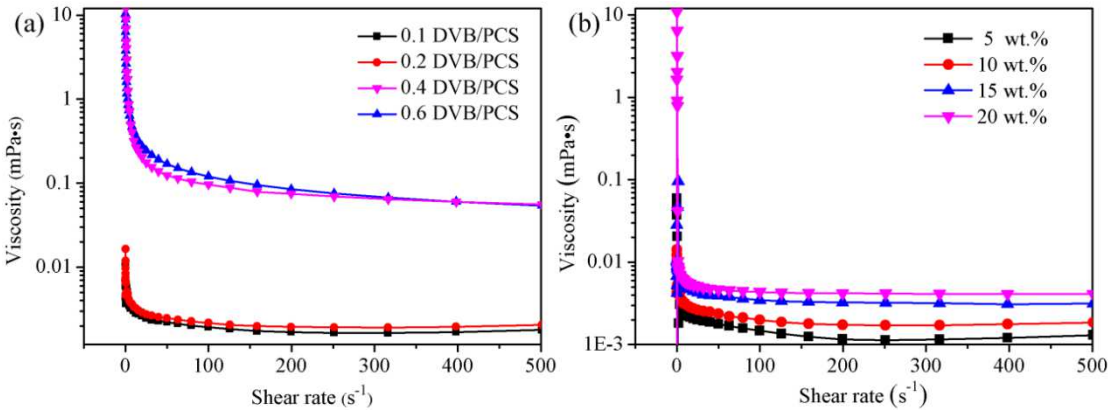

Fig. 2. Viscosities as a function of shear rate for DVB/camphene/PCS solution with various (a) DVB/PCS mass ratios and (b) PCS contents.

Fig. 3(a) shows images of freeze-dried samples before and after pyrolysis. Samples showed high integrity with 10 wt.% PCS and a 0.2 DVB/PCS mass ratio. After pyrolysis at 1200 °C, obvious shrinkage occurred with a linear shrinkage of approximately 45 %, as shown in Fig. 3(b). The colour changed from white to black on pyrolysis.

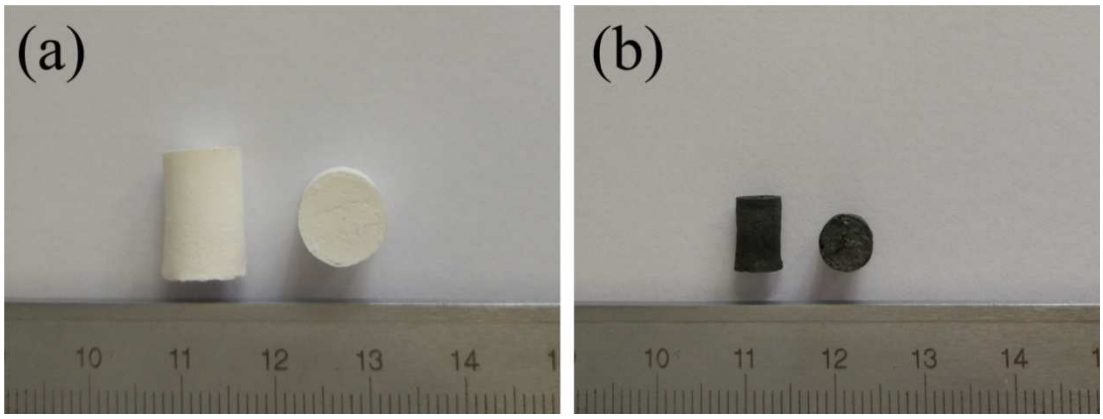

Fig. 3 Optical photographs of freeze cast samples (a) after freeze drying, (b) after pyrolysis at 1200 °C.

Fig. 4(a) and (c) show typical SEM micrographs of thermal-oxidation cured and cross-linked SiC samples prepared with 10 wt. % PCS after pyrolysis at 1200 °C. As shown in Fig. 4(a), the pore morphology replicates that of the frozen camphene solvent after sublimation, while the circular and dendritic pores, highlighted by yellow circles in Fig. 4, indicate the main crystal and dendritic arms [45, 46], respectively. During freeze casting, the PCS is squeezed out between the frozen camphene crystals, resulting in an amorphous β-SiC pore framework. On addition of DVB at a 0.2 DVB/PCS mass ratio, the morphology of the β-SiC porous structure changed, as shown in Fig.4(c). The dendritic arms became longer and many connecting bridges appeared between the secondary dendritic arms. The insets of Fig. 4(a) and (c) show detailed views of these secondary dendritic arms. Pyrolysis causes the pore size to reduce, as shown in the inset of Fig. 4(c).

Fig. 4(b) and (d) show the elemental analysis in randomly selected areas of two SiC samples obtained by thermal-oxidation and cross-linking curing, respectively. 6.2% mol. % oxygen was detected in the cross-linked cured sample, compared to 22.1 mol. % oxygen in the thermally-oxidized sample.

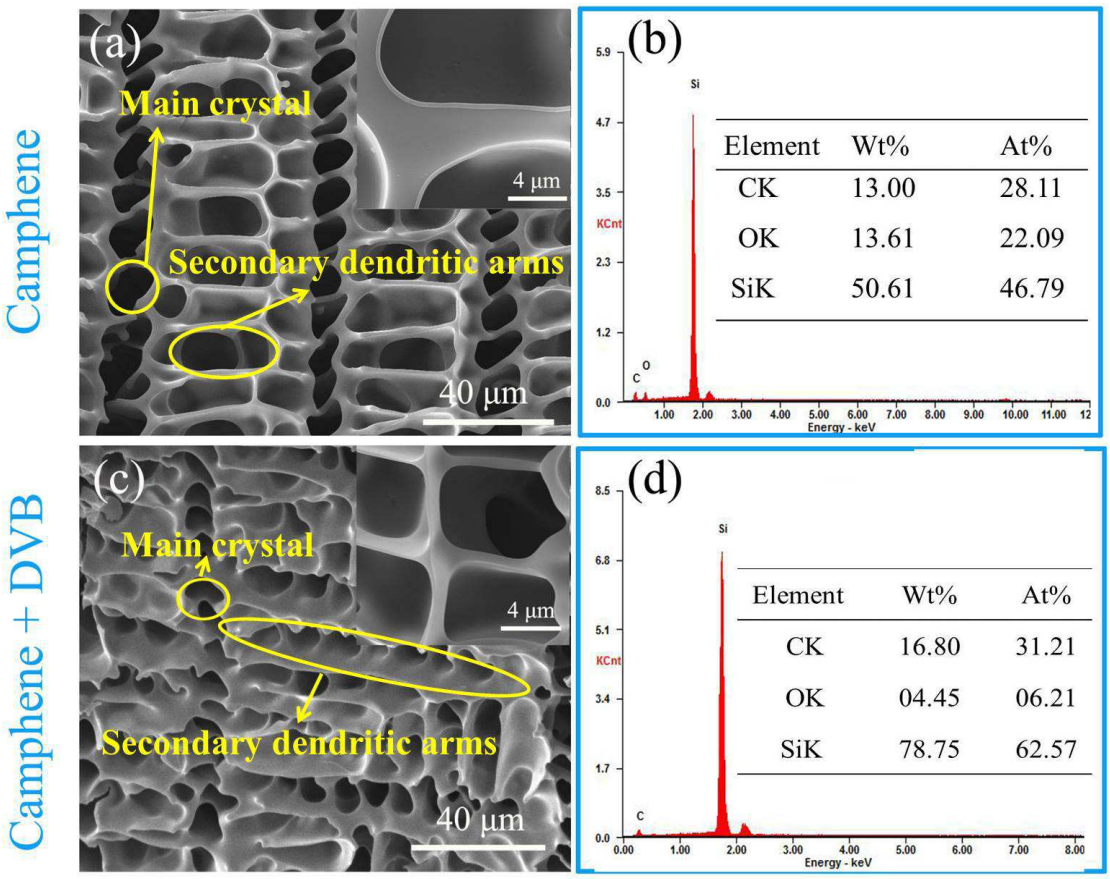

Fig. 4 (a) SEM images and (b) EDS data for porous SiC ceramics prepared by thermal oxidation curing; (c) SEM image and (d) EDS patterns of porous SiC ceramics with DVB cross-linking.

Fig. 5(a)-(d) show typical micrographs of pyrolyzed porous SiC prepared from solutions with various DVB/PCS mass ratios. The unidirectional freezing was perpendicular to the direction of the dendritic arms. The pore size was measured as the spacing between secondary dendritic arms and increased from about 9 μm to 21 μm as the DVB/PCS mass ratio increased from 0.1 to 0.6, respectively, while the width of the main crystal became larger with increasing DVB content. As the degree

of cross-linking increased, the dendritic arms disappeared, as shown in Fig. 5(d). The increased cross-linking in compositions with higher DVB content appears to prevent growth of camphene crystals during freeze casting, resulting in a microstructure dominated by the cross-linked PCS network.

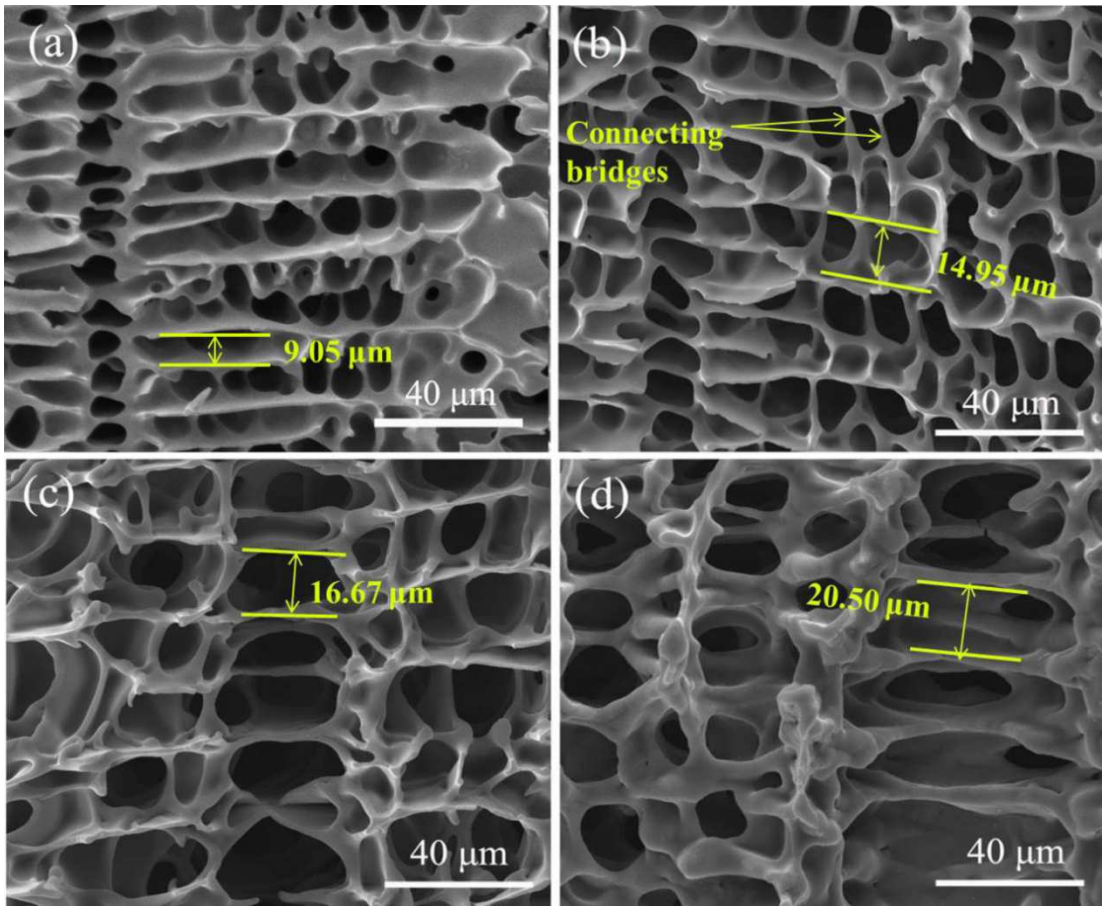

Fig. 5 Typical SEM images of freeze cast PCS after pyrolysis at 1200 °C, with (a) 0.1, (b) 0.2, (c) 0.4, (d) 0.6 DVB/PCS mass ratios. The unidirectional freezing was perpendicular to the secondary dendritic arms direction.

Fig. 6(a)-(d) show the microstructures of pyrolyzed porous SiC prepared from solutions with PCS contents ranging from 5 – 20 wt. %, with a constant DVB/PCS mass ratio of 0.2. The pore size decreased from about 16.1 µm to around 5.4 µm, with

PCS content increasing from 5 wt. % to 20 wt. %, respectively. This tendency was consistent with the rheological behaviour of the suspensions. The viscosity of prepared solutions increased with increasing PCS content, with pore size reducing with increasing viscosity.

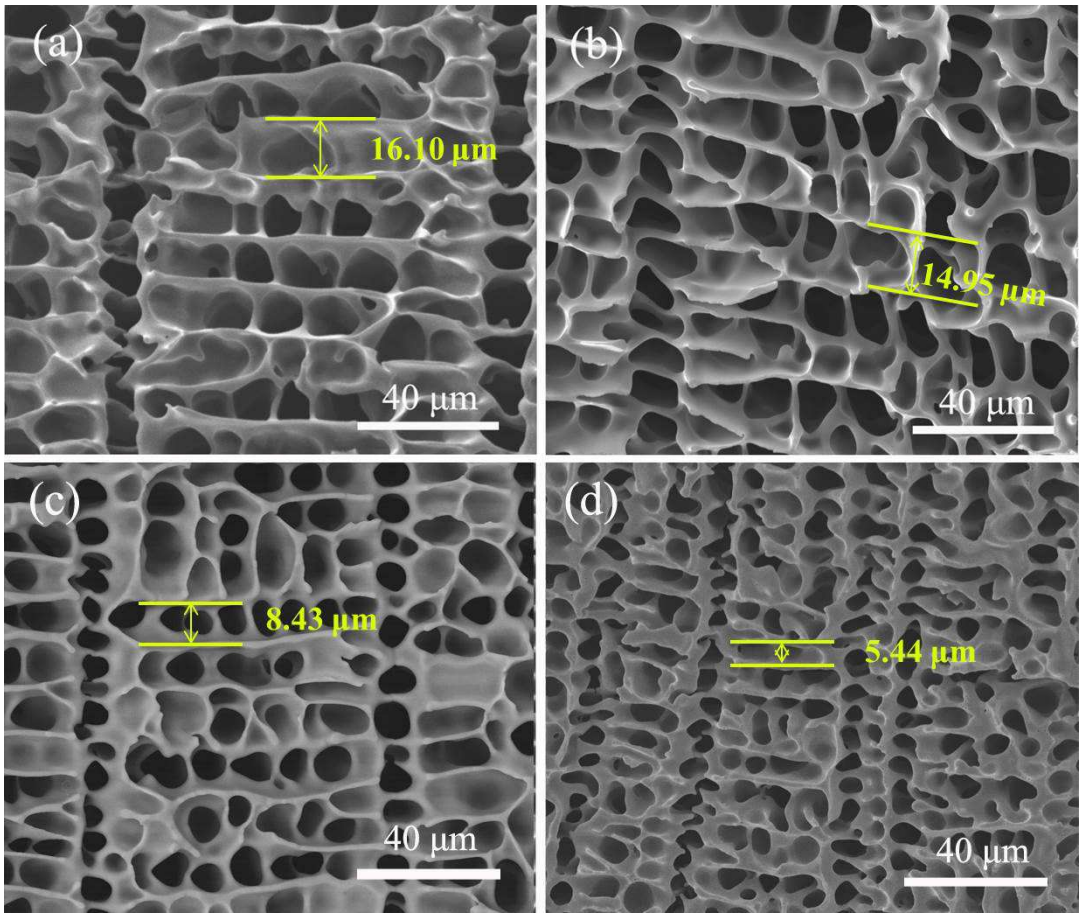

Fig. 6. Typical SEM images of freeze cast PCS with 0.2 DVB/PCS ratio after pyrolysis at 1200 °C, with (a) 5 wt. %, (b) 10 wt. % (c) 15 wt. % and (d) 20 wt. % PCS. The unidirectional freezing was perpendicular to the secondary dendritic arm direction.

Fig. 7 shows the FT-IR spectra of samples with different DVB/PCS mass ratios after

freeze drying, but before pyrolysis, compared with the spectrum of a pyrolyzed sample The observed bands matched well with those reported in the literature [25, 37]. All spectra show stretching peak at 795 cm^{-1} is assigned to Si-C bonds. For pure PCS, previous literature reported that when camphene was used as a solvent it did not alter the chemical structure of the PCS polymer [37]. Indeed, typical peaks for pure PCS are found in the spectrum of the uncross-linked PCS. For the cross-linked PCS samples, several additional weak peaks at 1434 cm^{-1} and 1643 cm^{-1} are observed in the spectra compared to that of the uncross-linked sample which originate from the bending vibration of the C=C bond in the aromatic ring of DVB. The Si-H absorption band at around 2100 cm^{-1} is weaker in the spectra of the cross-linked samples than in that of the uncross-linked PCS, due to hydrosilylation with the vinyl groups of DVB (Eqn 1), and on pyrolysis disappears completely, indicating conversion into the ceramic. Comparing the spectra of the cross-linked PCS samples, it is evident that the degree of cross-linking increases with increasing DVB content [42]. The results demonstrate that PCS was successfully converted into SiC ceramic after pyrolysis.

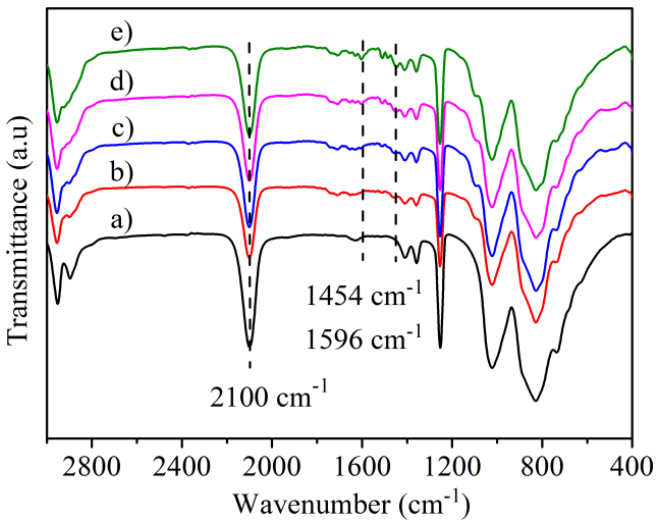

Fig. 7 FT-IR spectra of (a) to (e) studied samples prior to pyrolysis and (f) the 0.2 DVB/PCS sample after pyrolysis.

Fig. 8(a) and (b) show XRD patterns illustrating the crystallization of the PCS derived ceramics derived from solutions containing different DVB/PCS mass ratios ranging from 0.1 to 0.6 and various PCS mass fractions ranging from 5 wt. % to 20 wt. %, respectively. All samples exhibited a nanocrystalline structure. Broad characteristic peaks of β-SiC at 2θ = 35.7°, 60.0° and 72.0° are assigned to the (111), (220), (311) planes of this phase (PDF#01-1119) [37, 48] .

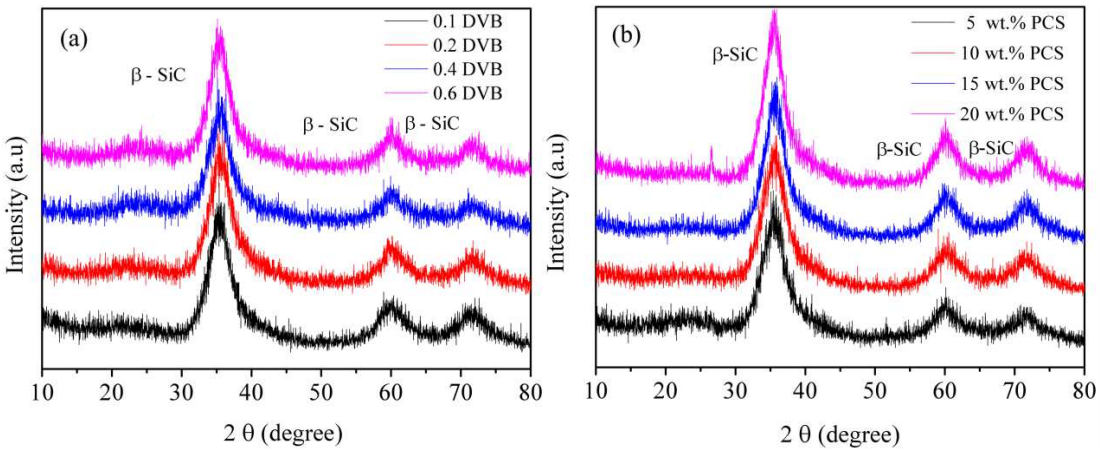

Fig. 8. XRD patterns of pyrolyzed PCS samples derived from different (a) DVB/PCS mass ratios and (b) PCS loadings.

Fig. 9 (a) shows the porosity and compressive strength of pyrolyzed SiC samples. The porosity increased from 82% to 85 % as the DVB/PCS mass ratio changed from 0.1 to 0.6. The compressive strength was highest for 0.2 DVB/PCS sample with a value of

9.9 MPa. Higher levels of DVB content, i.e. 0.4 and 0.6, led to stronger polymer gelation during the solution preparation and the freeze casting, which caused variation of the pore morphology and the corresponding compressive strength [49]. The 0.1 DVB/PCS sample had relatively low porosity; the shrinkage was not only larger for this sample, but it also failed to maintain its cylindrical shape. This is due to the fact that the extent of cross-linking was relatively low (the 0.1 DVB/PCS ratio corresponds to only around 9% of the stoichiometric maximum DVB/PCS ratio). In contrast, for the 0.2 DVB/PCS mass ratio sample (corresponding to around 18% of the stoichiometric maximum DVB/PCS ratio), the cylindrical shape was maintained.

Fig. 9 (b) shows the compressive strengths of pyrolyzed SiC samples prepared from the solutions with various mass fractions of PCS, revealing a clear improvement of the compressive strength with PCS content increasing from 5 wt. % to 20 wt. %. The highest compressive strength was 18.7 MPa for the 20 wt. % PCS sample. As shown in Fig.6, the pore size decreases with increasing PCS mass fraction, with porosity decreasing from 87% to 59% for PCS contents of 5 and 20 wt. %, respectively Low porosity and thicker dendritic structures favour higher compressive strength. The connecting bridges might also contribute to the improved compressive strength.

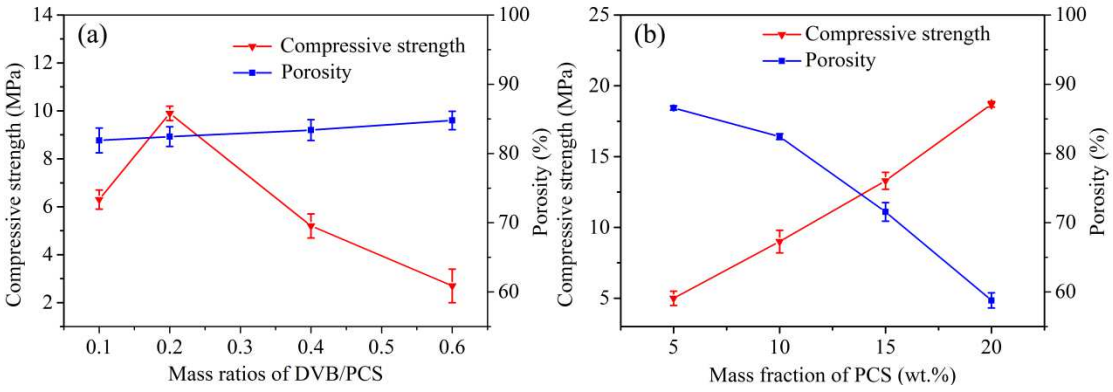

Fig. 9 Porosity and compressive strength of pyrolyzed PCS with (a) various DVB/PCS mass ratios with 10 wt.% PCS and various PCS contents at a 0.2 DVB/PCS mass ratio.

4. Conclusions

Porous silicon carbide (SiC) ceramics with low oxygen content were prepared by freeze casting using divinylbenzene (DVB) as a cross-linker for polycarbosilane (PCS). The effects of DVB content and PCS mass fraction on the solidification of PCS/camphene solutions were investigated. The dendritic arms of camphene became longer and many connecting bridges appeared between the secondary dendritic arms with increasing of DVB content. Cross-linking cured SiC ceramics with 6.21 mol. % oxygen were achieved, while the oxygen content increased to 22.09 mol. % in thermally-oxidized samples. At a 0.2 DVB/PCS ratio an optimum microstructure is achieved, reflecting that of the camphene solvent, including secondary dendritic arms. This leads to a maximum in compressive strength, ascribed to the increased number of SiC walls and the connecting bridge structures formed between adjacent secondary

dendritic arms. Changes in the microstructure at higher DVB result in lower compressive strengths. In addition, a clear improvement in compressive strength with increasing PCS content is seen, with the highest compressive strength of 18.7 MPa found for samples with 20 wt. % PCS and a 0.2 DVB/PCS mass ratio.

Acknowledgements

This work was financially supported by the National Natural Science Foundation of China (51672311), Science and Technology Project of Hunan Province, China (no. 2016WK2022), and Supported by the State Key Laboratory of Powder Metallurgy, Central South University, Changsha, China.

References:

[1] P. Greil, T. Lifka, A. Kaindl, Biomorphic Cellular Silicon Carbide Ceramics from Wood: I. Processing and Microstructure, J. Eur. Ceram. Soc. 18 (1998) 1961-1973.

[2] H. Ichikawa, F. Machino, S. Mitsuno, T. Ishikawa, K. Okamura, Y. Hasegawa, Synthesis of continuous silicon carbide fibre, J Mater Sci. 21 (1986) 4352-4358.

[3] Y. Ma, Q.S. Ma, J. Suo, Z.H. Chen, Low-temperature fabrication and characterization of porous SiC ceramics using silicone resin as binder, Ceram Int. 34 (2007) 253-255.

[4] J.M. Qian, Z.H. Jin, X.W. Wang, Porous SiC ceramics fabricated by reactive infiltration of gaseous silicon into charcoal, Ceram Int. 30 (2004) 947-951.

[5] G. Amirthan, A. Udayakumar, V.V.B. Prasad, M. Balasubramanian, Synthesis and

characterization of Si/SiC ceramics prepared using cotton fabric, Ceram Int. 35 (2009) 967-973.

[6] S.M. Manocha, H. Patel, L.M. Manocha, Effect of Steam Activation on Development of Light Weight Biomorphic Porous SiC from Pine Wood Precursor, J. Mater. Eng. Perform. 22 (2013) 396-404.

[7] M. Benaissa, J. Werckmann, G. Ehret, E. Peschiera, J. Guille, M.J. Ledoux, Structural studies of active carbon used in the growth of silicon carbide catalyst support, J Mater Sci. 29 (1994) 4700-4707.

[8] W. Yang, H. Miao, Z. Xie, L. Zhang, L. An, Synthesis of silicon carbide nanorods by catalyst-assisted pyrolysis of polymeric precursor, Chem. Phys. Lett. 383 (2004) 441-444.

[9] Q.G. Fu, H.J. Li, X.H. Shi, K.Z. Li, J. Wei, Z.B. Hu, Synthesis of silicon carbide nanowires by CVD without using a metallic catalyst, Mater. Chem. Phys. 100 (2006) 108-111.

[10] P. Pastila, V. Helanti, A.P. Nikkilä, T. Mäntylä, Environmental effects on microstructure and strength of SiC-based hot gas filters, J. Eur. Ceram. Soc. 21 (2001) 1261-1268.

[11] S. Schaafhausen, E. Yazhenskikh, S. Heidenreich, M. Müller, Corrosion of silicon carbide hot gas filter candles in gasification environment, J. Eur. Ceram. Soc. 34 (2014) 575-588.

[12] Z. Taslicukur, C. Balaban, N. Kuskonmaz, Production of ceramic foam filters for molten metal filtration using expanded polystyrene, J. Eur. Ceram. Soc. 27 (2007)

637-640.

[13] M. Fukushima, Y. Zhou, Y.I. Yoshizawa, Fabrication and Microstructural Characterization of Porous SiC Membrane Supports with Al_2O_3–Y_2O_3 Additives, J. Membr. Sci. 339 (2009) 78-84.

[14] S. Dabir, W. Deng, M. Sahimi, T. Tsotsis, Fabrication of Silicon Carbide Membranes on Highly Permeable Supports, J. Membr. Sci. 537 (2017) 239-247.

[15] M. Fukushima, Y. Zhou, H. Miyazaki, Y. ichi. Yoshizawa., K. Hirao, Y. Iwamoto, S. Yamazaki, T. Nagano, Microstructural Characterization of Porous Silicon Carbide Membrane Support With and Without Alumina Additive, J. Am. Ceram. Soc. 89 (2010) 1523-1529.

[16] S. Santavirta, M. Takagi, L. Nordsletten, A. Anttila, R. Lappalainen, Y.T. Konttinen, Biocompatibility of silicon carbide in colony formation test in vitro. A promising new ceramic THR implant coating material, Arch Orthop Trauma Surg. 118 (1998) 89-91.

[17] P.S.P. Anand, N. Arunachalam, L. Vijayaraghavan, Investigation on Grindability of Medical Implant Material Using a Silicon Carbide Wheel with Different Cooling Conditions , Procedia Manufacturing. 10 (2017) 417-428.

[18] A. Lloyd, P. Tobias, A. Baranzahi, P. Martensson, I. Lundstrom, Current status of silicon carbide based high-temperature gas sensors, IEEE Trans. Electron Devices. 46 (1999) 561-566.

[19] H.P. Phan, D.V. Dao, K. Nakamura, S. Dimitrijev, N.T. Nguyen, The Piezoresistive Effect of SiC for MEMS Sensors at High Temperatures: A Review, J.

Microelectromech. Syst. 24 (2015) 1663-1677.

[20] H. Zhang, J. Zhang, H. Zhang, Computation of radar absorbing silicon carbide foams and their silica matrix composites, Comput. Mater. Sci. 38 (2007) 857-864.

[21] J. She, J.F. Yang, N. Kondo, T. Ohji, S. Kanzaki, Z.Y. Deng, High□Strength Porous Silicon Carbide Ceramics by an Oxidation□Bonding Technique, J. Am. Ceram. Soc. 85 (2002) 2852-2854.

[22] S. Ding, S. Zhu, Y.P. Zeng, D. Jiang, Fabrication of mullite-bonded porous silicon carbide ceramics by in situ reaction bonding, J. Eur. Ceram. Soc. 27 (2007) 2095-2102.

[23] M. Kotani, K. Nishiyabu, S. Matsuzaki, S. Tanaka, Processing of polymer-derived porous SiC body using allylhydridopolycarbosilane (AHPCS) and PMMA microbeads, J Ceram Soc Jpn. 119 (2011) 563-569.

[24] T. Konegger, R. Patidar, R.K. Bordia, A novel processing approach for free-standing porous non-oxide ceramic supports from polycarbosilane and polysilazane precursors, J. Eur. Ceram. Soc. 35 (2015) 2679-2683.

[25] M. Fukushima, P. Colombo, Silicon carbide-based foams from direct blowing of polycarbosilane, J. Eur. Ceram. Soc. 32 (2012) 503-510.

[26] Y.W. Kim, C.B. Park, Processing of microcellular preceramics using carbon dioxide, Compos. Sci. Technol. 63 (2003) 2371-2377.

[27] L. Borchardt, M. Oschatz, S. Graetz, M.R. Lohe, M.H. Rümmeli, S. Kaskel, A hard-templating route towards ordered mesoporous tungsten carbide and carbide-derived carbons, Microporous Mesoporous Mat. 186 (2014) 163-167.

[28] S. Ungureanu, G. Sigaud, G.L. Vignoles, C. Lorrette, M. Birot, A. Derré, O. Babot, H. Deleuze, A. Soum, G. Pécastaings, Tough silicon carbide macro/mesocellular crack-free monolithic foams, J. Mater. Chem. A. 21 (2011) 14732-14740.

[29] E. Zera, R. Campostrini, P.R. Aravind, Y. Blum, G.D. Sorarù, Novel SiC/C Aerogels Through Pyrolysis of Polycarbosilane Precursors, Adv. Eng. Mater. 16 (2014) 814-819.

[30] S.C. Zunjarrao, A. Rahman, R.P. Singh, Characterization of the Evolution and Properties of Silicon Carbide Derived From a Preceramic Polymer Precursor, J. Am. Ceram. Soc. 96 (2013) 1869–1876.

[31] C. Liu, K. Li, H. Li, S. Zhang, Y. Zhang, X. Hou, Synthesis, characterization, and ceramization of a SiC–ZrC–C preceramic polymer precursor, J Mater Sci. 50 (2015) 2824-2831.

[32] C. Vakifahmetoglu, D. Zeydanli, P. Colombo, Porous polymer derived ceramics, Mater. Sci. Eng. R-Rep. 106 (2016) 1-30.

[33] S. Deville, E. Saiz, R.K. Nalla, A.P. Tomsia, Freezing as a path to build complex composites, Science, 311 (2006) 515-518.

[34] Y. Zhang, K. Zhou, Y. Bao, D. Zhang, Effects of rheological properties on ice-templated porous hydroxyapatite ceramics, Mater Sci Eng C Mater Biol Appl. 33 (2013) 340-346.

[35] K. Zhou, Y. Zhang, D. Zhang, X. Zhang, Z. Li, G. Liu, T.W. Button, Porous hydroxyapatite ceramics fabricated by an ice-templating method, Scr. Mater. 64 (2011)

426-429.

[36] H.X. Zhang, P.D. Nunes, M. Wilhelm, K. Rezwan, Hierarchically ordered micro/meso/macroporous polymer-derived ceramic monoliths fabricated by freeze-casting, J. Eur. Ceram. Soc. 36 (2016) 51-58.

[37] B.H. Yoon, E.J. Lee, H.E. Kim, Y.H. Koh, Highly Aligned Porous Silicon Carbide Ceramics by Freezing Polycarbosilane/Camphene Solution, J. Am. Ceram. Soc. 90 (2007) 1753–1759.

[38] M. Naviroj, S.M. Miller, P. Colombo, K.T. Faber, Directionally aligned macroporous SiOC via freeze casting of preceramic polymers, J. Eur. Ceram. Soc. 35 (2015) 2225-2232.

[39] M. Tsumura, Silicon-Based interpentratry polymer networks(IPNS) :sythesis and properties, Macromolecules, 31 (1998) 2716-2723.

[40] G.D. Sorarù, F. Dalcanale, R. Campostrini, A. Gaston, Y. Blum, S. Carturan, P.R. Aravind, Novel polysiloxane and polycarbosilane aerogels via hydrosilylation of preceramic polymers, J. Mater. Chem. A. 22 (2012) 7676-7680.

[41] G.A. Danko, R. Silberglitt, P. Colombo, E. Pippel, J. Woltersdorf, Comparison of microwave hybrid and conventional heating of preceramic polymers to form silicon carbide and silicon oxycarbide ceramics, J. Am. Ceram. Soc. 83 (2000) 1617-1625.

[42] M. Tsumura, T. Iwahara, Synthesis and properties of crosslinked polycarbosilanes by hydrosilylation polymerization, Polym. J. 31 (1999) 452-457.

[43] J. Seuba, S. Deville, C. Guizard, A.J. Stevenson, Mechanical properties and failure behavior of unidirectional porous ceramics, Sci Rep. 6 (2016) 1-11.

[44] J. Stein, In Situ Determination of the Active Catalyst in Hydrosilylation reactions using highly reactive Pt(0) catalyst precursors, J. Am. Chem. Soc. 121 (1999) 3693-3703.

[45] B.H. Yoon, E.J. Lee, H.E. Kim, Y.H. Koh, Highly aligned porous silicon carbide ceramics by freezing Polycarbosilane/Camphene solution, J. Am. Ceram. Soc. 90 (2007) 1753-1759.

[46] M. Naviroj, P.W. Voorhees, K.T. Faber, Suspension- and solution-based freeze casting for porous ceramics, J. Mater. Res., (2017) 1-11.

[47] H.Q. Ly, R. Taylor, R.J. Day, F. Heatley, Conversion of polycarbosilane (PCS) to SiC-based ceramic Part 1. Characterisation of PCS and curing products, J Mater Sci. 36 (2001) 4037-4043.

[48] H.Q. Ly, R. Taylor, R.J. Day, F. Heatley, Conversion of polycarbosilane (PCS) to SiC-based ceramic Part II Pyrolysis and characterisation, J Mater Sci. 36 (2001) 4045-4057.

[49] H. Zhou, R.N. Singh, Kinetics Model for the Growth of Silicon Carbide by the Reaction of Liquid Silicon with Carbon, J. Am. Ceram. Soc. 78 (1995) 2456-2462.